RESEARCH ARTICLE

Essential gene deletions producing gigantic bacteria

Jeannie Bailey[1], **Julie Cass**[2], **Joe Gasper**[1], **Ngoc-Diep Ngo**[1], **Paul Wiggins**[2], **Colin Manoil**[1] *

1 Department of Genome Sciences, University of Washington, Seattle, Washington, United States of America, **2** Department of Physics, University of Washington, Seattle, Washington, United States of America

* manoil@uw.edu

Abstract

To characterize the consequences of eliminating essential functions needed for peptidoglycan synthesis, we generated deletion mutations of *Acinetobacter baylyi* by natural transformation and visualized the resulting microcolonies of dead cells. We found that loss of genes required for peptidoglycan precursor synthesis or polymerization led to the formation of polymorphic giant cells with diameters that could exceed ten times normal. Treatment with antibiotics targeting early or late steps of peptidoglycan synthesis also produced giant cells. The giant cells eventually lysed, although they were partially stabilized by osmotic protection. Genome-scale transposon mutant screening (Tn-seq) identified mutations that blocked or accelerated giant cell formation. Among the mutations that blocked the process were those inactivating a function predicted to cleave murein glycan chains (the MltD murein lytic transglycosylase), suggesting that giant cell formation requires MltD hydrolysis of existing peptidoglycan. Among the mutations that accelerated giant cell formation after ß-lactam treatment were those inactivating an enzyme that produces unusual 3->3 peptide cross-links in peptidoglycan (the LdtG L,D-transpeptidase). The mutations may weaken the sacculus and make it more vulnerable to further disruption. Although the study focused on *A. baylyi*, we found that a pathogenic relative (*A. baumannii*) also produced giant cells with genetic dependencies overlapping those of *A. baylyi*. Overall, the analysis defines a genetic pathway for giant cell formation conserved in *Acinetobacter* species in which independent initiating branches converge to create the unusual cells.

Author summary

Although essential genes control the most basic functions of bacterial life, they are difficult to study genetically because mutants lacking the functions die. We have developed a simple procedure for creating bacteria in which different essential genes have been completely deleted, making it possible to analyze the roles of the missing functions based on the features of the dead cells that result. When genes needed for the production of the cell wall were inactivated, the bacteria formed bizarre giant cells. It was possible to identify the functions responsible for forming the giant cells, and to formulate a model for how they

form. Since cell wall synthesis is one of the most important antibiotic targets, understanding how bacteria respond to its disruption may ultimately help in developing procedures to overcome antibiotic resistant bacterial infections.

Introduction

In spite of controlling the most fundamental biological processes, essential genes are usually missing from loss-of-function mutant screens because strains carrying null mutations are not represented. Although essential functions can be studied using conditional alleles, such as temperature-sensitive or regulated expression alleles, suitable alleles that support normal growth under permissive conditions while fully eliminating activity under non-permissive conditions can be difficult to isolate [1, 2]. In the work reported here, we describe the use of gene deletions generated by natural transformation as an alternative to conditional alleles for studying essential functions. We employed the approach to examine the consequences of inactivating genes needed for peptidoglycan synthesis in *Acinetobacter baylyi*, a Gram-negative bacterium belonging to the Gammaproteobacteria [3]. We focused on peptidoglycan because it is the major determinant of cell shape and mutations affecting it can produce dramatically altered cell morphologies [4–6].

Peptidoglycan is an essential glycopeptide mesh situated between the two membranes of Gram-negative bacteria, which helps protect cells from lysis due to turgor pressure. Peptidoglycan is constructed by complex mechanisms in which a lipid-linked disaccharide pentapeptide precursor is incorporated into peptidoglycan through the action of transglycosylase and transpeptidase activities (Fig 1). Parallel sets of enzymes are required for cell elongation and division [7–11].

Peptidoglycan growth reflects a balance between synthetic and degradative activities [7, 8]. When new peptidoglycan biosynthesis is blocked, hydrolytic activities degrade the existing sacculus and bacteria usually lyse due to osmotic swelling. However, under osmoprotective conditions, cells are prevented from lysing and may proliferate as pleiomorphic wall-deficient cells called L-forms [12–15]. These bacteria have been an object of fascination for decades due to their capacity for growth without a peptidoglycan sheath, striking cell morphologies and antibiotic resistance [14, 15]. It appears that the formation of L-forms requires not only loss of peptidoglycan synthesis, but also additional mutations that allow the wall-deficient forms to proliferate by membrane tubulation and blebbing [5].

In some cases, loss of peptidoglycan synthesis leads not to L-forms, but to non-proliferating cells that have lost their normal shape and may enlarge considerably [5, 12, 13, 16–19]. For example, in one well-characterized example, mutations inactivating an *E. coli* cytoskeletal protein needed for elongation peptidoglycan synthesis (MreB) indirectly inactivate division by sequestering a division protein (FtsZ) in internal membranes [13], leading to giant cells. In other cases, blocking peptidoglycan synthesis converts the bacteria into small non-dividing spherical cells [16, 17, 20]. In *Vibrio cholera*, formation of such spheroids requires murein endopeptidase activity [16]. The small spherical cells can grow when peptidoglycan synthesis resumes; their formation thus represents a novel antibiotic tolerance mechanism. Genetic determinants of this tolerance have been defined [20].

In this study, we examined the consequences of disrupting peptidoglycan synthesis in *Acinetobacter baylyi*. There are several advantages of studying peptidoglycan synthesis in this bacterium. First, the species undergoes natural transformation at high efficiency [21, 22], making it straightforward to generate deletion mutations in essential genes. Second, peptidoglycan

PRECURSOR SYNTHESIS
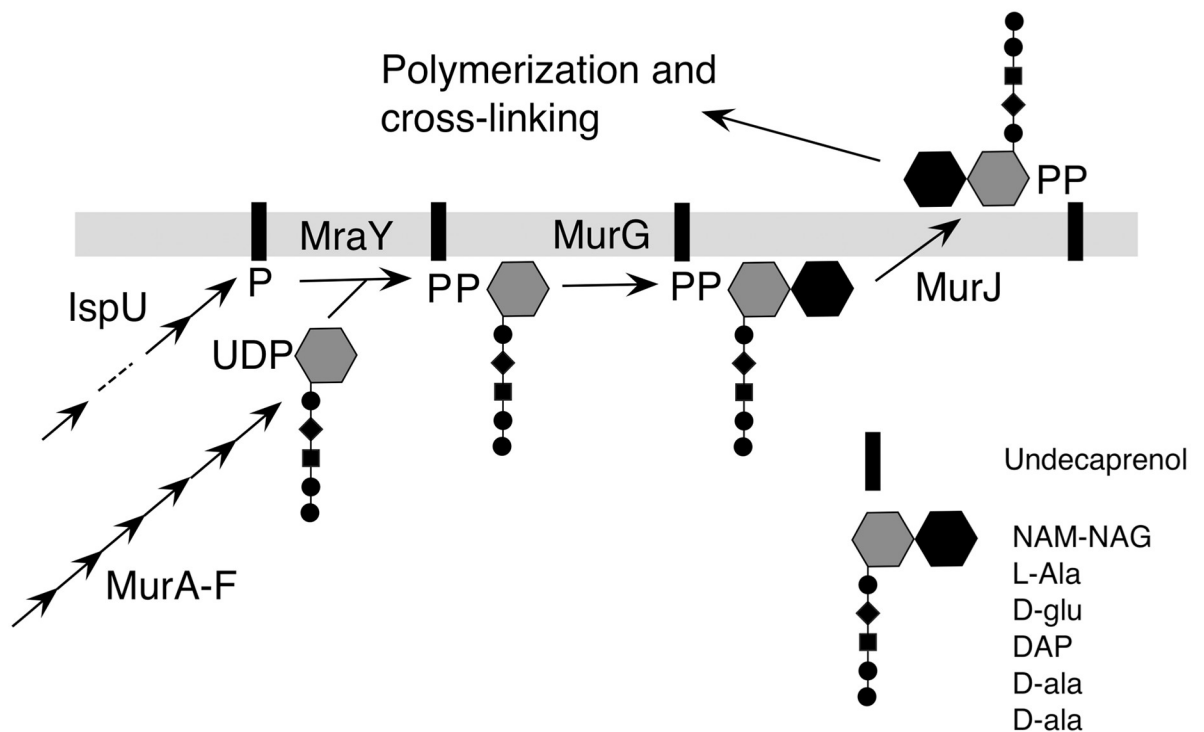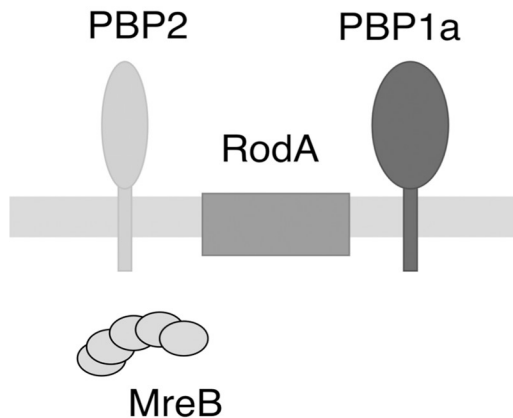
PRECURSOR INCORPORATION
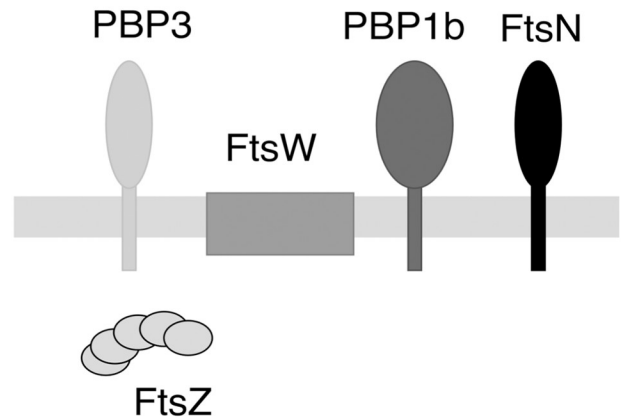
Fig 1. Peptidoglycan synthesis. Top panel, pathway of precursor undecaprenol disaccharide pentapeptide synthesis. Bottom panel, key functions in peptidoglycan elongation and septal synthesis [11]. NAM-NAG, N-acetyl muramyl-N-acetyl glucosamine; PBP2 (PbpA) and PBP3 (FtsI), transpeptidases; RodA and FtsW, transglycosylases; PBP1a (PonA) and PBP1b (MrcB), transglycosylase-transpeptidases; FtsN, division regulator; MreB and FtsZ, cytoskeletal proteins.

synthesis associated with cell elongation is fully dispensable, making it simple to genetically manipulate septal synthesis in the absence of elongation synthesis. Third, like *E. coli*, *A. baylyi* belongs to the Gammaproteobacteria, and the detailed understanding of peptidoglycan synthesis and cell division in *E. coli* should provide a good foundation for understanding the processes in *A. baylyi*. Finally, *A. baylyi* peptidoglycan metabolism should be similar to that of the related nosocomial pathogen *Acinetobacter baumannii*. Understanding the consequences of disrupting peptidoglycan synthesis in *A. baylyi* may thus suggest approaches for enhancing the efficacy of antibiotics targeting the process in its clinically relevant relative.

We found that *A. baylyi* forms giant cells in response to a variety of deletion mutations and antibiotics blocking peptidoglycan synthesis. We exploited the powerful genetic analysis possible in *A. baylyi* to characterize the requirements for formation of giant cells and to formulate a pathway for their creation.

Results and discussion

Essential gene deletion mutations

We sought to characterize the cellular consequences of disrupting conserved essential processes like peptidoglycan synthesis. To do this, we generated essential gene deletions by natural transformation of *A. baylyi* and examined the cells that resulted. Bacteria were exposed to PCR DNA fragments that replace targeted genes with a kanamycin resistance determinant, followed by plating on agar containing kanamycin (Fig 2) (Materials and methods). Transformed cells incorporate the mutagenic DNA, deleting the corresponding essential gene, and then grow and divide, depleting the essential product. Proliferation stops when cells run out of the targeted essential gene product. The resulting microcolonies are made up of dead cells whose morphologies reflect loss of the targeted essential product, and whose size reflects how rapidly depletion of the product blocks growth. Typically 5–10% of the cells are transformed to generate deletions in such experiments, and kanamycin-sensitive untransformed cells are readily distinguished because they stop dividing largely as singlets and doublets with vegetative cell morphology (see below). The principle unwanted background event in the generation of essential gene deletions (occurring at ~10^{-6} frequency) appeared to be due to transformation of partially diploid cells (presumably due to tandem duplications), which generated fast growing cells carrying copies of both deletion and wild type alleles of targeted genes (Materials and methods) [23–26].

Mutations blocking peptidoglycan precursor synthesis lead to the formation of giant cells

In a large-scale screen of microcolonies of cells carrying deletion mutations affecting different essential processes, the most dramatic phenotypes resulted from disruption of peptidoglycan synthesis (Fig 1). For example, when the gene encoding the first step of lipid-linked disaccharide pentapeptide precursor synthesis (*murA*) was deleted by transformation with a Δ*murA::kan* PCR fragment, microcolonies of polymorphous giant cells formed (Fig 3). The giant cells were stabilized by high osmolarity medium and typically enlarged for ~12–24 hours. Giant cells also formed when wild-type bacteria were treated with fosfomycin, an antibiotic that targets MurA (see below). Giant cells could reach diameters greater than ten times that of vegetative cells (see below), and often contained one or more vacuoles at their peripheries (Fig 3, 12 and 24 h). The vacuoles failed to fluoresce in cells expressing cytoplasmic green fluorescent protein (S1 Fig), indicating that they are shielded from the cytoplasm, e.g., as if they were derived from the periplasm. Developing giant cells were sometimes joined to each other by
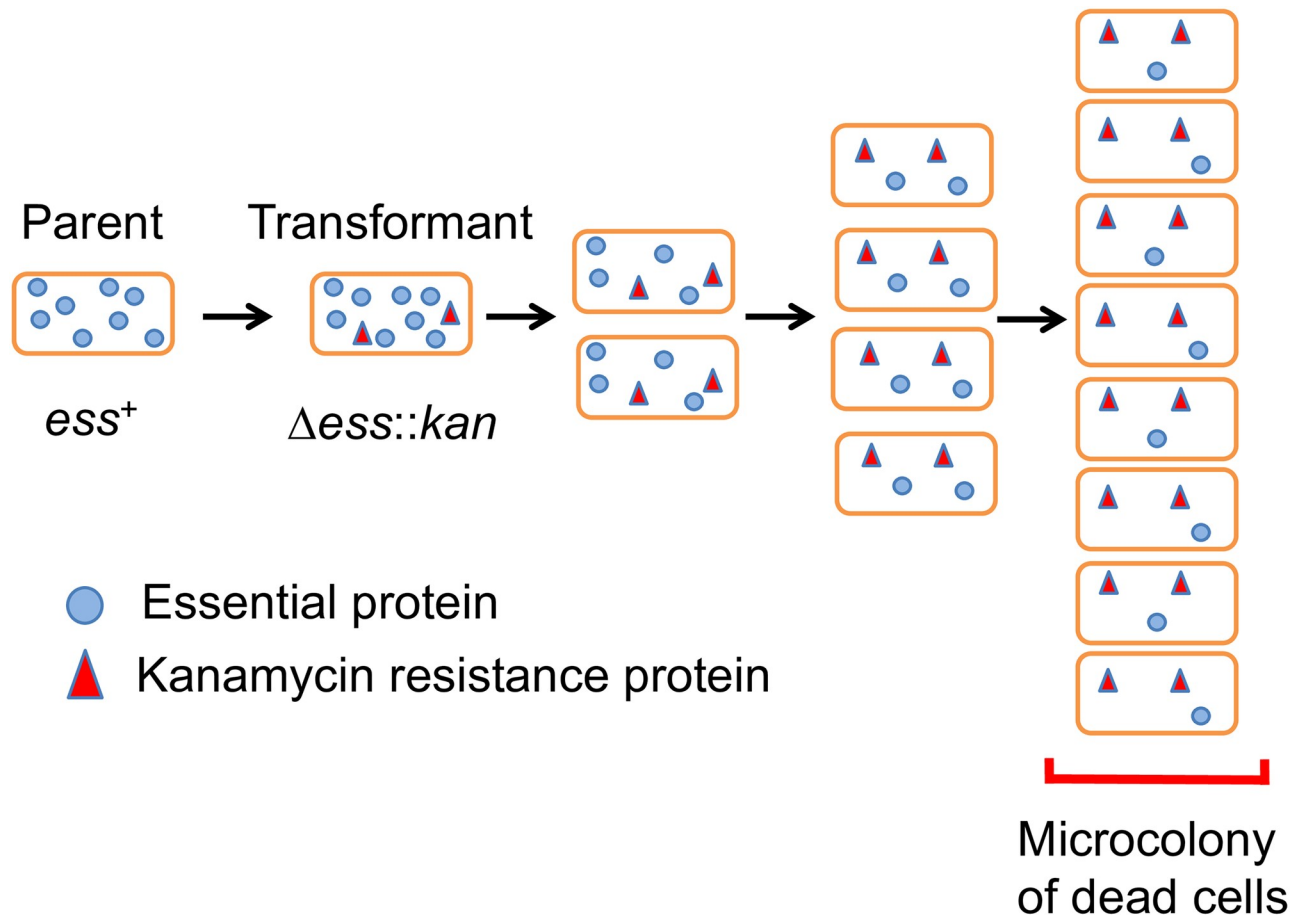
Fig 2. Cellular depletion of an essential product following gene deletion. Replacement of an essential gene with a kanamycin resistance marker allows growth and division of cells on agar medium supplemented with kanamycin until the essential product is sufficiently depleted to block further growth. The properties of the microcolony of dead cells that results reflect the phenotypic consequences of the deletion mutation. *ess*, essential gene; *kan*, kanamycin resistance determinant.

membranous bridges (Fig 3, 8 h bottom panel) or exhibited wispy filaments with vesicles extending from their surfaces (S1 Fig). The giant cells did not proliferate, and thus are distinct from L forms.

Time-lapse imaging of giant cell formation following *murA* deletion shows a process in which cells transform from rods into amorphous amoeboid cells that enlarge and eventually burst (S1 Movie). The development of the giant cells proceeds by enlargement without apparent midcell (preseptal) blebbing [27].

Deletions of other genes required for peptidoglycan precursor biosynthesis also produced microcolonies of giant cells (Fig 4A). The microcolonies appeared similar in wild type (wt) and in a peptidoglycan elongation–minus triple mutant genetic background ("ΔE") (see below). Mutations in three of the genes (*murG*, *murJ* and *mraY*) led to microcolonies similar in size to those produced by Δ*murA* mutants. The deletion of the fifth gene (*ispU*), required for cofactor undecaprenol synthesis, led to larger microcolonies than the others. Since undecaprenol is recycled rather than consumed by peptidoglycan synthesis, it may require more growth to deplete it than the precursor intermediates, leading to the larger mutant microcolonies. Overall, the results indicate that disrupting peptidoglycan precursor synthesis at different
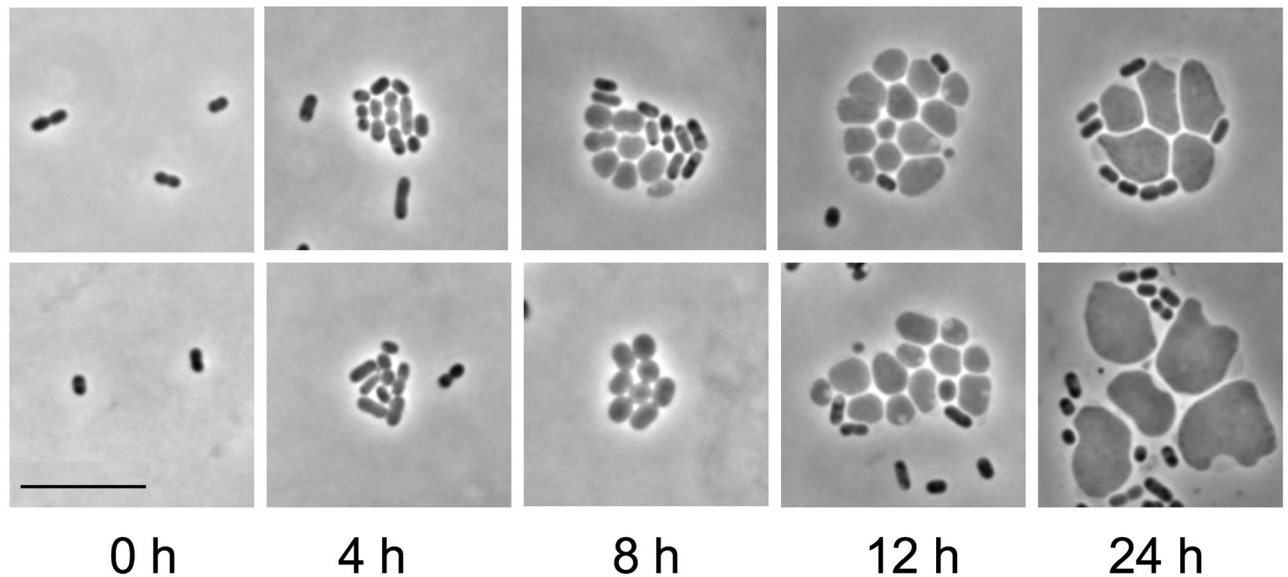
Fig 3. Microcolonies of giant cells formed after *murA* deletion. Two representative fields of developing microcolonies at different times following deletion of *murA* from wild type (MAY101) are shown. Cells were transformed with a Δ*murA*::*kan* PCR fragment, followed by incubation on agarose pads containing protective medium and kanamycin. Giant cell microcolonies usually contained some cells with vegetative cell dimensions. Such cells may originate from transformants that carried multiple copies of the *murA* locus (e.g., in multiple or partially replicated chromosomes), not all of which incorporated a Δ*murA*::*kan* fragment. Scale bar, 10 μm.

https://doi.org/10.1371/journal.pgen.1008195.g003

steps has a similar consequence, the formation of small microcolonies of giant cells. This phenotypic consistency suggests that intermediates in the peptidoglycan precursor synthetic pathway are not particularly toxic, in contrast, for example, to the lipopolysaccharide biosynthetic pathway [28].

Mutations blocking peptidoglycan precursor polymerization also produce giant cells

The lipid-linked disaccharide pentapeptide precursor is incorporated into peptidoglycan through the action of transglycosylase and transpeptidase activities, with different machineries responsible for cell elongation and division (Fig 1) [7]. Enzymes making up the elongation complex are nonessential in *A. baylyi*, although elongation–minus mutants grow as spheres rather than short rods [25]. Septal peptidoglycan synthesis functions are essential in *A. baylyi*. To evaluate whether blocking disaccharide pentapeptide precursor incorporation into peptidoglycan led to giant cell formation, we created mutants defective in both elongation and septal peptidoglycan synthesis. These strains were created from a parent ("ΔE"; MAY106) carrying deletion mutations eliminating three elongation functions (PBP2, RodA and PBP1a), combined with different mutations blocking cell division (Fig 4B). In all cases, elimination of elongation and division functions together led to the formation of giant cells, whereas the division mutations alone led to long filaments (Fig 4B). The results show that like eliminating precursor synthesis, disrupting incorporation of the precursors into peptidoglycan produces giant cells.

Antibiotics targeting peptidoglycan synthesis also induce giant cell formation

We also examined whether treating cells with antibiotics targeting peptidoglycan synthesis produced giant cells. In agreement with the mutant studies, we found that antibiotics
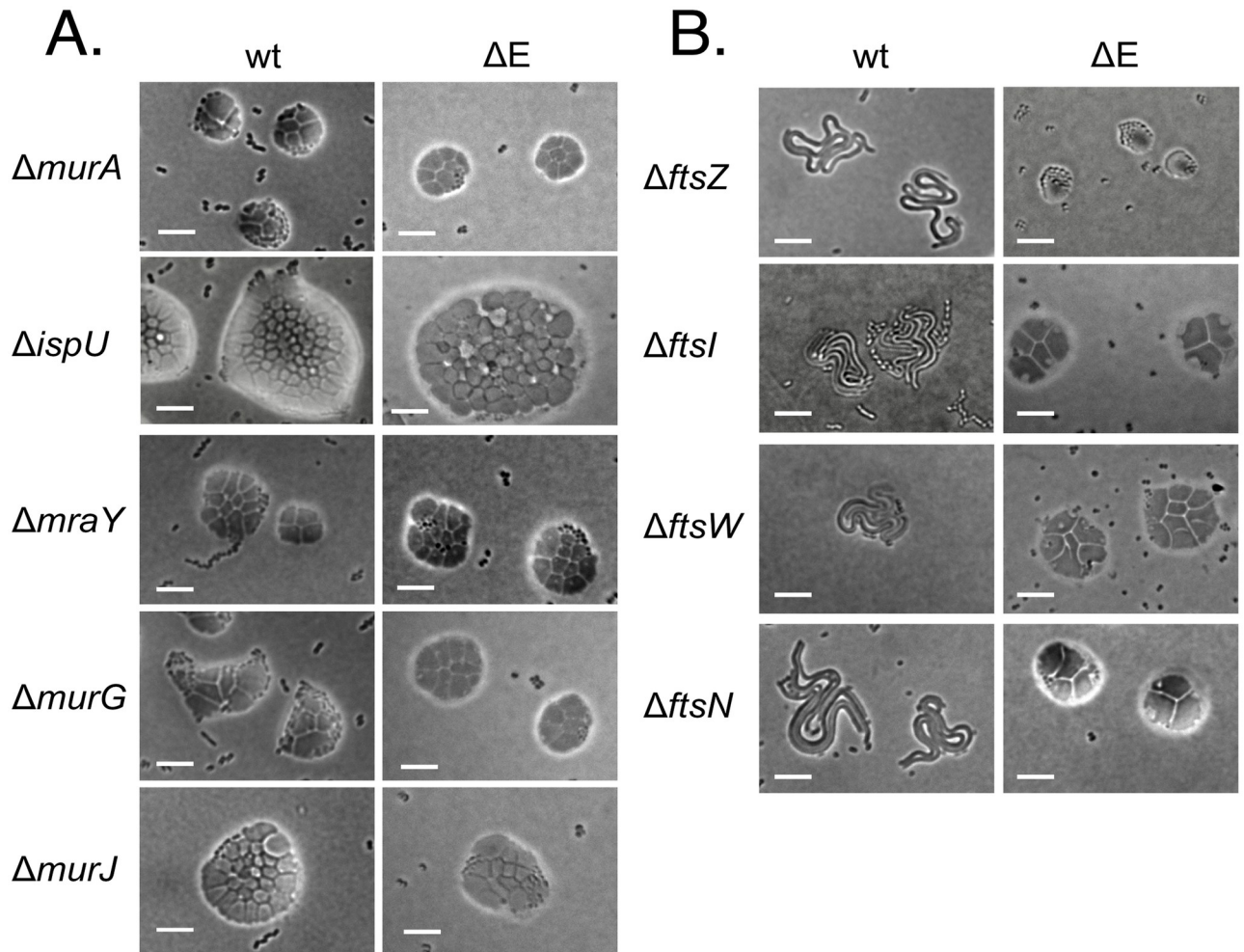
Fig 4. Blocking peptidoglycan precursor synthesis or polymerization leads to giant cells. A, Precursor synthesis mutants. Microcolonies formed after deletion of genes required for different steps of peptidoglycan precursor synthesis are shown. Deletions of *meso*-diaminopimelic acid synthesis genes *dapA* and *dapB* also resulted in giant cells. Colonies were incubated 20–24 h on protective agar. Scale bar, 10 μm. **B, Microcolonies of cell division mutants.** Microcolonies formed after deletion of genes required for cell division are shown. Colonies were incubated 20–24 h on protective agar. wt, wild-type (MAY101) genetic background; ΔE, peptidoglycan elongation-minus triple mutant (*ΔpbpA ΔrodA ΔponA*) genetic background (MAY106). Scale bar, 10 μm.

https://doi.org/10.1371/journal.pgen.1008195.g004

inhibiting precursor synthesis or peptide cross-linking induced giant cells (Fig 5). The antibiotics examined were fosfomycin, which targets MurA, aztreonam, which targets the division-specific transpeptidase FtsI (PBP3), and meropenem, which apparently targets both the PbpA (PBP2) and FtsI (PBP3) transpeptidases [29]. As expected, fosfomycin and meropenem treatments induced giant cells in both wild type and in an elongation-minus genetic background, whereas aztreonam induced giant cells only in the elongation-minus background. For all three antibiotic treatments, the giant cells were comparable in size, with median dimensions ~10 times that of untreated cells (Table 1).

Treatments with two additional antibiotics, cycloserine, which targets Ddl (D-ala-D-ala racemase) and Alr (alanine racemase), and the ß-lactam mecillinam, which apparently targets multiple cross-linking enzymes in *A. baylyi* (unlike in *E. coli*) [11], also led to giant cells. The findings indicate that, as was seen for deletion mutations, antibiotic inhibition of peptidoglycan precursor synthesis or incorporation into the sacculus produces giant cells.
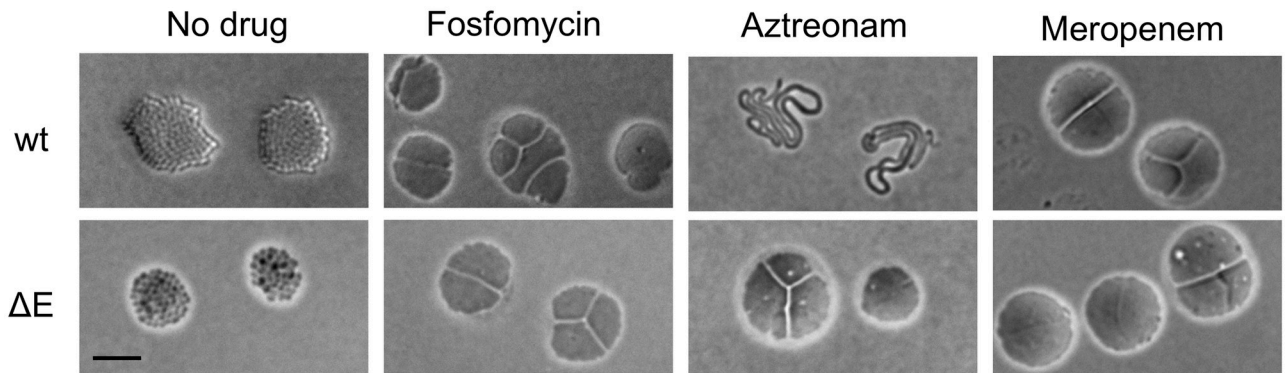
Fig 5. Antibiotic treatments producing giant cells. Microcolonies were grown on protective agar containing the indicated antibiotics (24 h) or no drug (11 h). The antibiotic concentrations are: fosfomycin (192 μg/ml), aztreonam (192 μg/ml) and meropenem (5 μg/ml). WT, wild type (MAY101); ΔE, peptidoglycan elongation-minus triple mutant (MAY106). Scale bar, 10 μm.

https://doi.org/10.1371/journal.pgen.1008195.g005

Mutations altering giant cell formation

A straightforward model for giant cell formation is that after inhibition of peptidoglycan synthesis blocks cell enlargement, the activity of hydrolytic functions ruptures the peptidoglycan sheath, allowing the growing cytoplasm to break out of it and expand [5, 13]. To identify functions potentially involved in this process, we screened for mutations altering giant cell recovery using saturation-level transposon mutant sequencing (Tn-seq). We assumed that the representation of mutations that either blocked or accelerated giant cell formation and subsequent lysis would be changed compared to growth without giant cell induction.

We carried out the screens after inducing giant cell formation by fosfomycin or aztreonam treatment (Materials and methods). For the fosfomycin treatment screens, we created a genome saturation-level mutant pool in wild type by transposon-transposase complex electroporation mutagenesis [30]. The pool was exposed to fosfomycin on protective medium to induce giant cells, and DNA isolated from the cells after 24 h growth was subjected to Tn-seq (Materials and methods). Mutations in 35 genes reduced recovery and in 56 genes increased recovery in the presence of fosfomycin compared to no antibiotic (S1 Database). A second set of Tn-seq screens employed a *ΔpbpA* (PBP2) mutant pool created by natural transformation of the wild-type pool used for the fosfomycin screen by *ΔpbpA*::kan (Materials and methods). The *ΔpbpA* mutant pool was exposed to aztreonam on protective medium, and DNA isolated at two different times for Tn-seq. In these screens, mutations in 54 genes reduced recovery and in 27 genes increased recovery relative to no treatment (S1 Database). Among the mutations depleted in one or both screens were those inactivating peptidoglycan penicillin binding proteins, recycling functions, and other proteins involved in peptidoglycan metabolism.

Table 1. Giant cell size. Dimensions of untreated cells or cells grown for 20–24 hr, 30˚ C, on protective agar containing fosfomycin (192 μg/ml), aztreonam (192 μg/ml) (*pbpA* deletion mutant), or meropenem (10 μg/ml) were measured. Isolated cells or cells in small microcolonies (≤4 cells) were included. W, width; L, length; D, diameter.

Treatment	Median size (μm)	Range (μm)	Number
None (WT)	0.6 (W) X 1.2 (L)	0.4–0.9 (W) X 0.8–2.1 (L)	100
None (ΔpbpA)	1.2 (D)	0.7–1.6 (D)	100
Fosfomycin (WT)	9.3 (D)	1.8–13.7 (D)	82
Aztreonam (ΔpbpA)	12.1 (D)	2.9–15.3 (D)	55
Meropenem (WT)	8.2 (D)	2.9–12.6 (D)	150

https://doi.org/10.1371/journal.pgen.1008195.t001

Two caveats in interpreting the phenotypes of transposon insertion mutants are that strains may carry unlinked mutations, and that insertions may have polar effects on downstream genes in operons. Unlinked mutations responsible for phenotypes are unlikely in our analysis because the phenotypes identified in the Tn-seq screens are seen for multiple independent insertions (>35/gene on average). In most cases, polar effects are also unlikely to account for mutant phenotypes, because the saturation-level genome coverage Tn-seq provides includes all of the (nonessential) genes in an operon. Thus, a polar effect would be seen as a downstream gene (as well as the upstream gene) having a mutant phenotype. Although there were four such genes in our top set, validation studies for three of them with constructed mutants designed to be nonpolar indicate that their phenotypes were not due to polarity (next section).

Validation of Tn-seq findings

Since Tn-seq assays involve cells grown in competition, weak growth phenotypes can lead to significant mutant representation changes. To distinguish the subset of genes with strong mutant phenotypes, we carried out validation experiments with individual mutants. We constructed and analyzed 38 deletion mutants corresponding to genes identified in the Tn-seq screens (32/38) or considered candidates based on their annotated functions (6/38). The mutations were created by replacing the targeted genes with a kanamycin resistance determinant oriented the same as the deleted gene to support transcription of any downstream genes and reduce polar effects [1] (Materials and methods). A total of 29 of the 38 deletions were confirmed to affect giant cell formation (S1 Table), eleven of them leading to particularly strong phenotypes (Table 2).

Mutations in four of the eleven genes blocked giant cell formation at intermediate stages. Deletions of two of the four (*mrcB*, encoding transglycosylase-transpeptidase PBP1b, and *lpoB*, encoding an MrcB regulator) [31], had similar phenotypes, leading to much stronger defects in fosfomycin induction than aztreonam induction, with intermediate effects on meropenem induction (Fig 6). The mutations blocked fosfomycin induction at an early stage at which cells rounded but did not enlarge significantly before lysing. Deletions of the other two genes (*mltD*, encoding a membrane lytic transglycosylase, and *gcf (*g̲iant c̲ell f̲ormation), encoding an exported protein of unknown function) blocked induction by all three antibiotics. However, the phenotypes differed depending on the condition. The blocks in fosfomycin induction were severe, with modest but detectable enlargement before lysis. In contrast, both mutations allowed more enlargement following aztreonam and meropenem induction, producing clusters of "small giants". Bridges between cells in such clusters were common. Similar clusters were seen as an intermediate in the formation of giant cells after aztreonam treatment of the ΔPBP2 strain.

Mutations in four other genes accelerated giant cell formation and lysis. Mutations in three of them were specific to aztreonam induction (*ldtG*, encoding a peptidoglycan DAP-DAP (3->3) cross-linking enzyme; *dacA*, encoding peptidoglycan carboxypeptidase PBP5; and *ponA*, encoding transglycosylase-transpeptidase PBP1a) (S2 Fig). We suspected that the mutations may lead to a weakened peptidoglycan with reduced cross-linking that is more sensitive to further reduction upon aztreonam exposure. Indeed, all three mutations reduced the aztreonam minimal inhibitory growth concentration (MIC) (S2 Fig legend). Mutations in a fourth gene (*nagZ*, encoding a peptidoglycan recycling function) led to a complex phenotype. They affected fosfomycin induction more strongly than aztreonam induction, with some early giant cell formation and rampant lysis (S3 Fig). Other recycling pathway mutants also reduced giant cell recovery in Tn-seq (S1 Database). The recycling pathway provides a precursor that

Table 2. Mutations altering giant cell formation. The genes with the strongest mutant phenotypes among the deletion mutants examined (S1 Table) are listed. The number/total Tn-seq runs in which mutants in the indicated genes were significantly depleted or enriched are indicated. PBP, penicillin binding protein; nd, not determined due to low representation in the ΔPBP2 transposon mutant pooled library; wt, wild type.

Locus	Gene	Product	Fosfomycin (wt)		Aztreonam (ΔPBP2)	
			Tn-seq recovery	Deletion phenotype	Tn-seq recovery	Deletion phenotype
ACIAD0527	gcf	Sel1 domain	Decreased (2/2)	Fails to form giant cells, early lysis	nd	Early lysing clusters of small giant cells
ACIAD0551	nagZ	N-acetyl-ß-glucosaminidase	Decreased (2/2)	Early forming, early lysing giant cells	Decreased (7/8)	Slightly early lysing giant cells
ACIAD1138	mltD	Lytic transglycosylase	Decreased (2/2)	Fails to form giant cells, early lysis	–	Early lysing small giant cells
ACIAD1225	dacA	PBP5	–	Forms giant cells	Decreased (8/8)	Early forming, early lysing giant cells
ACIAD1396	–	Histidine triad protein	Increased (2/2)	Late forming, late lysing giant cells	Increased (8/8)	Partial resistance
ACIAD2234	mrcB	PBP1b	Decreased (2/2)	Fails to form giant cells, early lysis	Decreased (2/8)	Early forming, early lysing giant cells
ACIAD2235	lpoB	PBP1b activator	Decreased (2/2)	Fails to form giant cells, early lysis	Decreased (1/8)	Forms giant cells
ACIAD2336	zapE	Divisome ATPase	Increased (2/2)	Late forming, late lysing giant cells	Increased (8/8)	Partial resistance
ACIAD2475	ldtG	L, D-transpeptidase	–	Forms giant cells	Decreased (8/8)	Early forming, early lysing giant cells
ACIAD3361	ponA	PBP1a	–	Forms giant cells	Decreased (7/8)	Early forming, early lysing giant cells
ACIAD3380	ettA	Translation regulator	Increased (2/2)	Late forming stable giant cells	Increased (5/8)	Partial resistance

https://doi.org/10.1371/journal.pgen.1008195.t002
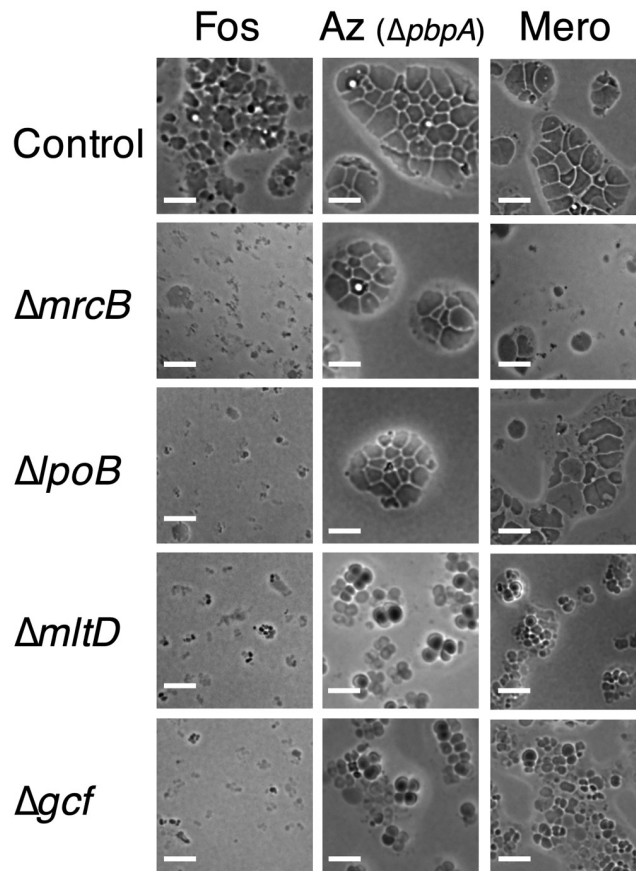
Fig 6. Mutations blocking giant cell formation in *A. baylyi*. The microcolonies formed by mutants blocked in giant cell formation on protective agar containing antibiotics inducing giant cell formation are shown. Mutations were in the wild type genetic background (MAY101) for the fosfomycin and meropenem treatments and in the PBP2⁻ (ΔpbpA) genetic background (MAY102) for the aztreonam assays. Control, ΔIS (MAY116); Fos, fosfomycin (360 μg/ml); Az, aztreonam (192 μg/ml); Mero, meropenem (10 μg/ml). Scale bar, 10 μm.

https://doi.org/10.1371/journal.pgen.1008195.g006

bypasses the fosfomycin-inhibited step of the *de novo* pathway (MurA). As thus expected, the *nagZ* mutation reduced the fosfomycin MIC (S3 Fig legend).

Most mutations increasing Tn-seq recovery moderately to severely reduced vegetative growth rate and may simply delay giant cell lysis by slowing down progression through the pathway (S1 Database). Three examples of such genes with strong mutant phenotypes were *ettA*, encoding a regulator of translation, *ACIAD1396*, encoding a histidine triad protein of unknown function, and *zapE*, encoding a division ATPase (Table 2). We did not identify any mutations allowing giant cells to propagate as L forms.

In the course of these validation experiments, we identified an unusual phenotype associated with loss of *zipA*, a gene encoding a division protein that is essential in *E. coli* but not in *Acinetobacter* species [32]. A Δ*zipA* mutation alone caused *A. baylyi* cells to propagate as elongated rods, some very long (S4 Fig). When a Δ*zipA* mutation was combined with a mutation blocking elongation peptidoglycan synthesis (ΔPBP2), the double mutant bacteria propagated as mixed colonies of enlarged spherical cells and giant cells (S4 Fig). We suspect that the *zipA* mutation hobbles septal peptidoglycan synthesis such that Δ*zipA* ΔPBP2 double mutant cells divide less frequently than ΔPBP2 mutant alone, leading to larger spheres, and that occasional outright division failure in the double mutant leads to the production of the giant cells.

Lipooligosaccharide-minus mutants form fragile giant cells

Acinetobacter species produce an outer membrane lipooligosaccharide (LOS) that corresponds to lipopolysaccharide lacking an O side chain [33]. Since the outer membrane contributes significantly to envelope stability [34], we sought to examine whether lipooligosaccharide (LOS) is needed for giant cell formation. Although LOS is nonessential in *Acinetobacter* species [33], its absence slows growth and the corresponding mutants were poorly represented in the transposon mutant pools we used for Tn-seq analysis. To test the requirement for LOS in *A. baylyi* giant cell formation, we therefore generated deletions of genes required for LOS precursor synthesis (*lpxA*) or transport to the outer membrane (*lptAB*). Both classes of mutations affected giant cell formation. The LpxA mutant, which grew as enlarged spheres without antibiotic, formed giant cells after fosfomycin treatment that frequently lysed earlier than usual (S5 Fig). The LptAB deletion mutant grew as smaller spheres and had a more dramatic defect, with massive lysis under giant cell induction conditions. Recent studies have found that LOS transporter mutations cause toxic precursors to accumulate in cells [28, 35], and we suspect the Δ*lptAB* phenotype may be accentuated by such toxicity. Overall, the studies thus indicate that the loss of LOS does not block giant cell formation, but that the cells formed are more fragile than those of wild type.

Reverse phenocopy test

If the antibiotics that induce giant cell formation act by inhibiting their established targets (MurA for fosfomycin and FtsI (PBP3) for aztreonam), inducing giant cells by deleting the target genes should show the same genetic dependencies as those seen for antibiotic induction. To test this prediction, we examined whether three of the mutations blocking giant cell formation after antibiotic treatment also blocked it after deletion of the target genes. We saw congruent effects in all three cases (S6 Fig), a result supporting the conclusion that the two antibiotics induce giant cells by inhibition of their established targets.

Survival assay

The mutations blocking fosfomycin-induced giant cell formation appeared microscopically to cause early, wholesale lysis (Fig 6). In order to quantify this lysis and death, we exposed

bacteria grown in liquid protective medium to fosfomycin and followed recovery of viable bacteria (colony forming units) (Fig 7). Under these conditions, the wild type and a control mutant (carrying a neutral kanamycin resistance marker) exhibited good recovery for eight hours, whereas five mutants defective in forming giant cells all showed >100-fold reductions in recovery. The mutants and wild type showed comparable growth and survival in the absence of fosfomycin. The results indicate that unimpaired giant cell formation helps protect cells from rapid death when peptidoglycan precursor synthesis is blocked, i.e., contributes to fosfomycin tolerance.

Giant cell formation in *Acinetobacter baumannii*

Is the response of *A. baylyi* to inhibition of peptidoglycan synthesis seen for other *Acinetobacter* species? A previous study by Doerr et al. found that meropenem treatment of a clinical isolate of the nosocomial pathogen *A. baumannii* converted the bacteria into non-dividing spheres that resemble small giant cells [16]. We examined giant cell formation by *A. baumannii* strain AB5075, and found that like *A. baylyi*, the strain formed giant cells upon exposure to fosfomycin or meropenem (Fig 8). In addition, transposon insertion mutants in *mrcB* (ABUW_1358), *mltD* (ABUW_2840) and *gcf* (ABUW_3408) interfered with the process in a manner similar to that seen for *A. baylyi*, albeit more weakly for fosfomycin induction (Fig 8). The finding that *A. baumannii* forms giant cells upon inhibition of peptidoglycan synthesis with some of the same genetic dependencies as *A. baylyi* suggests that the processes are similar in the two species.

Giant cell formation pathway

Our results make it possible to formulate a genetic pathway for giant cell formation in *A. baylyi* (Fig 9). The pathway is initiated by blocking either the *de novo* biosynthesis of peptidoglycan precursor (upper left) or incorporation of the precursor into the existing murein sacculus (lower left), with convergence of the two initiating branches. The biosynthesis block can be achieved by null mutations in genes encoding biosynthetic enzymes or by an antibiotic that targets one of the enzymes (fosfomycin, inhibiting MurA). The precursor incorporation block can be achieved in the absence of elongation synthesis by null mutations in division genes or treatment with an antibiotic targeting septal peptidoglycan synthesis (aztreonam, inhibiting FtsI).

Other mutations accelerate giant cell formation but do not induce it. Inactivating a peptidoglycan recycling gene (*nagZ*) accelerates their formation and lysis after fosfomycin treatment, presumably because recycling provides an intermediate later in the precursor biosynthetic pathway than the product of the MurA step [36, 37]. Mutations inactivating three genes (*ldtG*, *dacA* and *ponA)* accelerate giant cell formation following inhibition of precursor incorporation (aztreonam treatment of an elongation-minus mutant). LdtG shows homology to enzymes (L,D-transpeptidases) that produce an unusual class of peptide cross-links (DAP--DAP) in peptidoglycan [38, 39], and reducing their level could accelerate giant cell formation by making cells more sensitive to loss of the more abundant cross-links (DAP-D-ala). DacA is a carboxypeptidase that is needed in *E. coli* to provide the substrate for L,D-transpeptidase [40], and may play an analogous role in *A. baylyi*. In *E. coli*, the transglycosylase activity of MrcB (PBP1B) is also required for L,D-transpeptidase-dependent growth, and the *ponA* (PBP1A) transglycosylase might play an analogous role in *A. baylyi*.

Mutations in four genes block giant cell formation following initiation. Two of the genes are relatively specific for the precursor synthesis branch (*mrcB* and *lpoB*), with mutants rounding up and lysing without enlarging significantly following initiation. The *mrcB* gene encodes a transglycosylase-transpeptidase (PBP1b), whereas the *lpoB* gene encodes an outer membrane
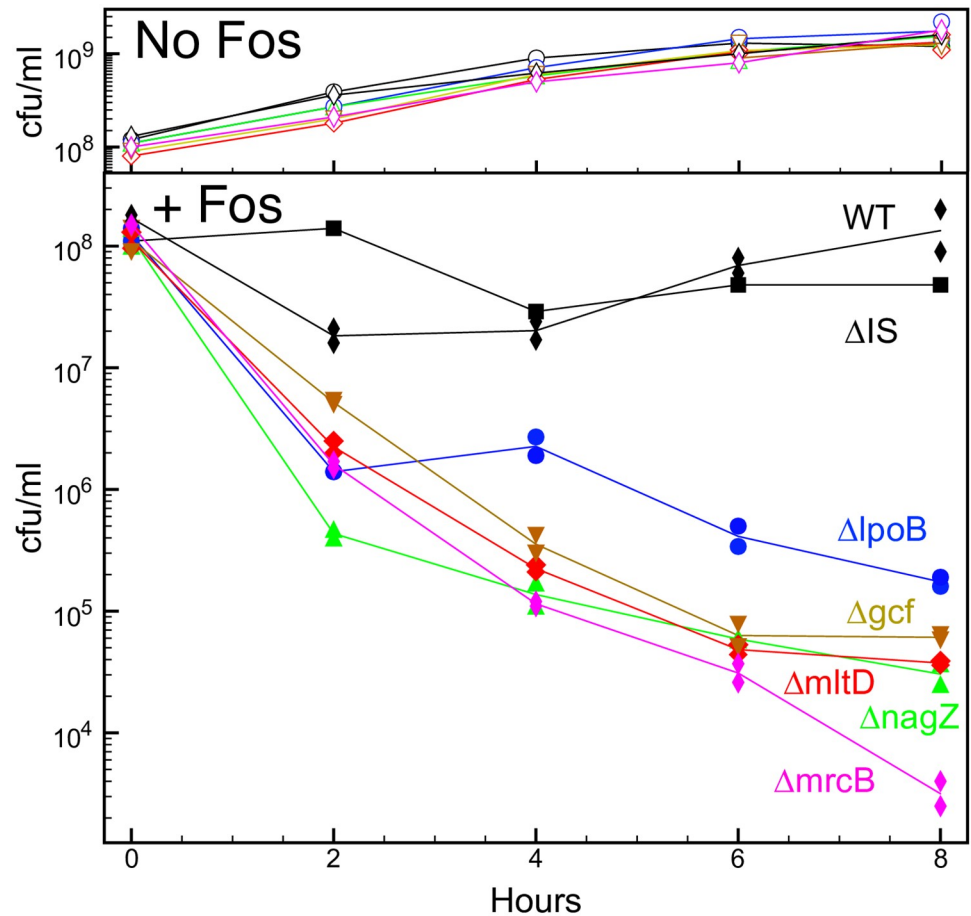
Fig 7. Fosfomycin killing of giant cell-minus mutants. The survival of bacteria in liquid protective medium following exposure to fosfomycin (192 µg/ml) was assayed. Wild type cells exposed to fosfomycin in liquid medium were smaller and less prone to lysis than on agar medium. The killing assays were carried out in duplicate for all strains except MAY116, and geometric means are plotted. The median geometric standard deviation for duplicates was 1.2, and in all cases was less than 1.8. WT, MAY101; ΔIS, MAY116; Δ*lpoB*, MAY114; Δ*gcf*, MAY108; Δ*mltD*, MAY110; Δ*nagZ*, MAY125; Δ*mrcB*, MAY113. cfu, colony-forming units; FOS, fosfomycin.

https://doi.org/10.1371/journal.pgen.1008195.g007

protein that activates PBP1b [31]. In *E. coli*, PBP1b is needed for the generation of L forms [15, 41] and the conversion of spheroplasts to vegetative cells [42], indicating that the protein stabilizes peptidoglycan-deficient cells. The protein may thus also stabilize early intermediates in *A. baylyi* giant cell formation when precursor synthesis is blocked. Mutations in two other genes alter giant cell induction by both initiation branches of the pathway (*mltD*, *gcf*). However, the blocks are different for the two modes of initiation. When precursor synthesis is blocked, the mutants enlarge somewhat and then lyse. When precursor incorporation is blocked, they form small giant cells that also have a tendency to lyse. The *mltD* gene encodes a membrane lytic transglycosylase predicted to hydrolyze the peptidoglycan glycan backbone. MltD activity may contribute to giant cell formation by allowing the growing cytoplasm to emerge from the constraining murein sacculus when new peptidoglycan synthesis is blocked. We think it is unlikely that MltD carries out a function analogous to Slt in *E. coli* of selective elimination of uncrosslinked precursors [11] because it is needed for giant cell induction when precursor synthesis is blocked. Gcf is a protein of unknown function, but is predicted to be an exported protein with a Sel1 tetratricopeptide protein interaction module [43]. Perhaps Gcf interacts with and
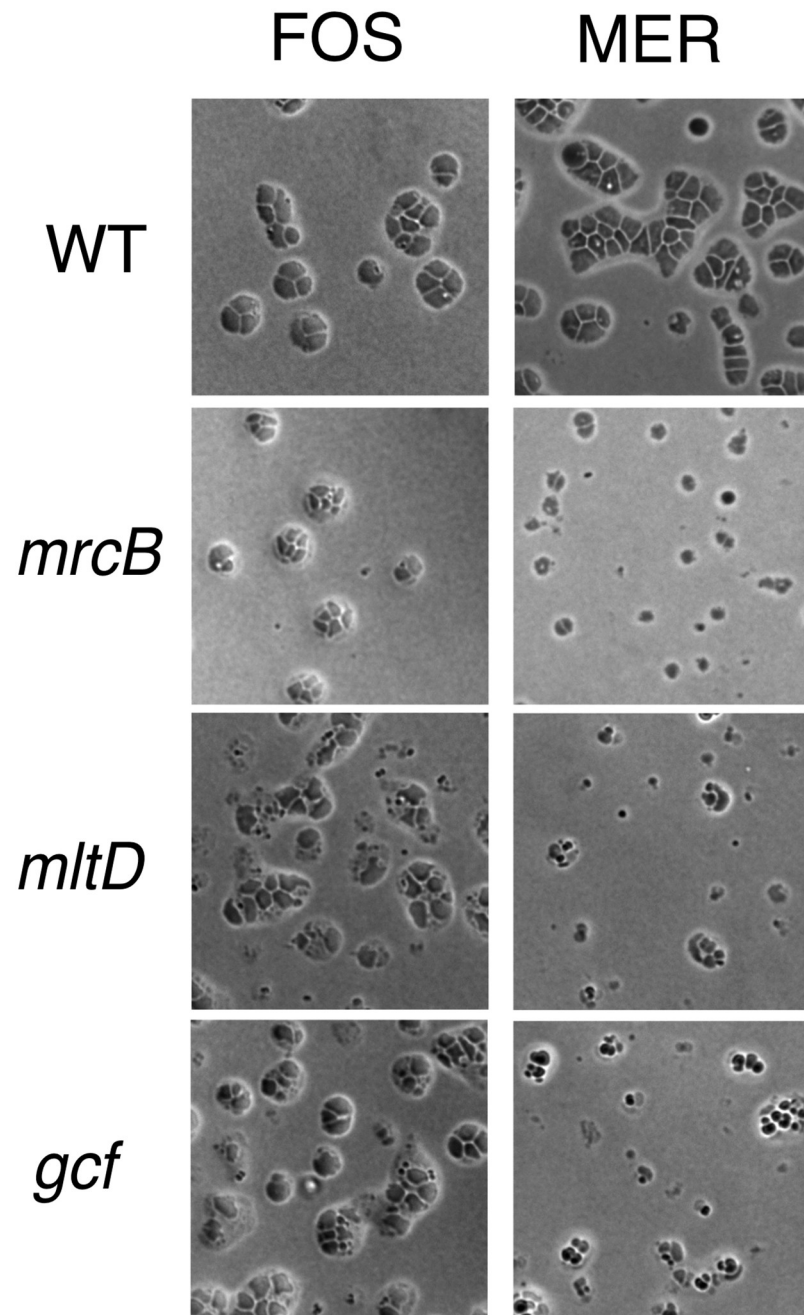
Fig 8. Giant cell formation by *A. baumannii*. *A. baumannii* strain AB5075 and the indicated transposon mutants were exposed to fosfomycin (192 μg/ml) (FOS) or meropenem (25 μg/ml) (MER) on protective agar and incubated for 8 hr at 37 ˚C. prior to imaging. WT, AB5075-UW; Δ*mrcB*, AB03662; *mltD*, AB07437; *gcf*, AB08926.

activates MltD. A Δ*gcf* Δ*mltD* double mutant exhibits a giant cell induction defect no greater than that of a Δ*mltD* single mutant, supporting this possibility.

It remains to be determined how well the *Acinetobacter* pathway for giant cell formation represents the generation of wall-deficient forms of other bacteria. However, an intriguing potential link to the recovery of peptidoglycan-deficient *V. cholerae* spheroids is provided by the observation that a lytic transglycosylase (MltA) is required for the process [20].
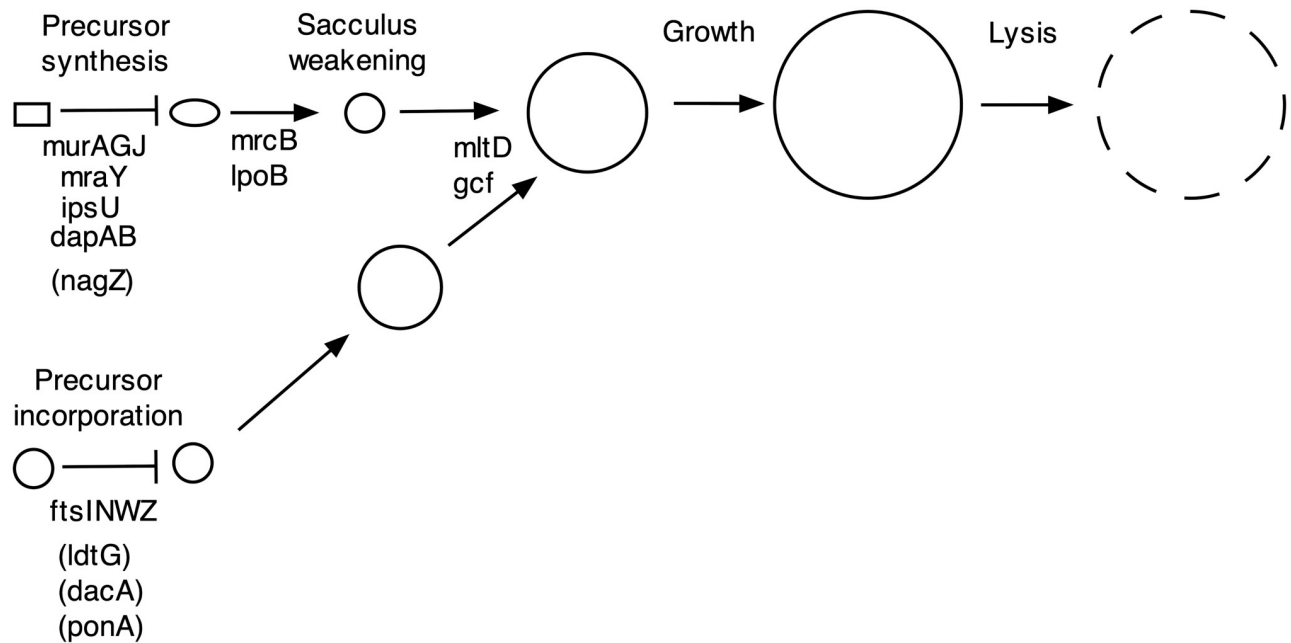
Fig 9. Giant cell formation pathway for *A. baylyi*. The pathway is initiated by mutations (or antibiotics) inactivating peptidoglycan precursor synthesis (upper branch) or polymerization (lower branch). The branches then converge with formation of giant cells and their eventual lysis. Mutations in genes in parentheses accelerate giant cell formation but do not induce it. Mutations that block the pathway at intermediate steps (*mrcB*, *lpoB*, *mltD* and *gcf*) also increase lysis.

Giant cells *versus* L forms

What is the relationship between giant cells and L forms? Both types of cells result from inhibition of peptidoglycan synthesis and are pleomorphic, but L forms proliferate and giant cells do not. We hypothesize that giant cells represent a primary consequence of growth without peptidoglycan synthesis, and that additional mutations are required for them to proliferate as L forms. This model readily accounts for overlap in functions needed for production of the two types of cells (e.g., *mrcB*) and the low yield of L forms when peptidoglycan synthesis is inhibited (e.g., ~10^{-5}–10^{-4}/cell) [41]. Natural variation in the capacity of different bacteria to generate L forms may reflect differences in other factors needed for L form growth, e.g., the nature and amount of polysaccharide capsule [41, 44].

Conclusion

In this study we used a new procedure for examining the terminal phenotypes of bacteria deleted of essential genes to analyze mutations disrupting peptidoglycan synthesis. Mutations blocking the process in different ways led to the formation of pleomorphic giant cells, and the phenotypes of mutants defective in making the unusual cells suggested a genetic pathway for their formation.

Materials and methods

Strains and growth media

Mutant strains were derivatives of *Acinetobacter baylyi* ADP1 (MAY101) [3] (the gift of C. Harwood) and *A. baumannii* AB5075-UW [45]. *A. baylyi* MAY106 ("ΔE") (*ΔpbpA ΔrodA*

Δ*ponA*) is an unmarked peptidoglycan elongation-deficient triple mutant constructed from ADP1. *A. baylyi* MAY116 is a "wild type" control strain carrying a kanamycin resistance marker (*nptII*) in place of an IS element (IS1236_1) [3, 24]. MAY103 carries a Δ*pbpA* allele marked with *nptII*. A complete list of strains is provided in S2 Database.

Growth media were TYE (10 g tryptone, 5 g yeast extract, 8 g sodium chloride and 15 g agar per liter), LB (TYE lacking agar) and minimal-succinate (M9 medium [46] supplemented with 15 mM sodium succinate, 2 mM magnesium sulfate, 0.1 mM calcium chloride and 1–3 μM ferrous sulfate ±15 g agar/l. Protective medium was minimal-succinate supplemented with 0.4 M sucrose and 10 mM magnesium sulfate, and was solidified with 1.5% agar ("protective agar") or 2% agarose ("protective agarose"). Supplements were routinely used at the following concentrations: kanamycin, 10 μg/mL (TYE) or 20μg/mL (minimal media); fosfomycin, 192–360 μg/mL; aztreonam, 120–190 μg/mL; and meropenem, 5–25 μg/mL. *A. baylyi* strains were routinely grown at 30˚ C whereas *A. baumannii* strains were grown at 37˚ C.

Construction of deletion mutations

We created deletion mutations by natural transformation of linear DNA fragments constructed by PCR using extension overlap [22, 47, 48]. The transformed fragments carried sequences of homology of ~2 kb flanking targeted genes that were either directly joined (for unmarked deletions) or flanked a kanamycin resistance determinant (for *kan*-marked deletions). Unmarked deletions were in-frame and included 18 bp insertions carrying diagnostic restriction sites at the deletion junctions. Marked deletions carried the *nptII* gene ("*kan*") from plasmid pACYC177 [49] encoding kanamycin resistance, with *nptII* in the same orientation as the deleted gene. In creating deletions, we designed primers (and often employed the same primers) as described previously [25] (S2 Database). Thermocycling reactions employed Q5 Polymerase (New England Biolabs), and DNA fragments were routinely purified using Qiaquick columns (Qiagen) prior to transformation.

The mutagenic DNA fragments were transformed into *A. baylyi* cultures grown overnight in minimal-succinate with 1uM ferrous sulfate, diluted 1:5 in fresh medium and grown one hour with shaking at 30˚. DNA was added at 1μg/mL, followed by incubation for 3 hours with shaking and plating on selective (marked deletions) or non-selective (unmarked deletions) media. Unmarked deletion mutations were identified by screening individual colonies by PCR using primers flanking targeted genes. Essential gene *kan*-marked deletion mutations were selected by plating on protective medium containing kanamycin (20 μg/mL). All unmarked and the majority of marked deletion mutations were verified by PCR. Microcolonies of the deletion mutants were generally imaged after 18–24 hours incubation at 30˚ C. In a typical experiment creating *kan*-marked essential gene deletions, 5–10% of the cells were transformed forming microcolonies of cells carrying the deletion. There was commonly a background of ~10^{-6} fast-growing colonies that carried both deleted and undeleted versions of the targeted genes [25], presumably arising from cells with tandem duplications.

Microscopy

Bacterial microcolonies were routinely imaged after growth on protective agar in 15 X 60 mm diameter Petri plates under bright field illumination using a Nikon Eclipse 90i with an ELWD 20X objective equipped with 2X digital zoom. For high-resolution imaging, microcolonies were grown on thin 2% agarose protective medium pads under cover slips in Gene Frames (Thermo Scientific) prior to phase contrast imaging using a 100X oil immersion objective. The microcolonies of giant cells grown in Gene Frames tended to be somewhat smaller and lyse somewhat earlier than those formed on plates.

Transposon mutagenesis

ADP1 was mutagenized by insertion of the tetracycline resistance-marked transposon T26 using a modification of a previously described procedure [45]. An overnight LB culture of ADP1 was diluted 1:200 into fresh medium without NaCl and grown with shaking to OD600 0.8. Cells were then pelleted and washed three times in decreasing volumes of cold 10% glycerol until cells had been concentrated approximately 150-fold. Aliquots (~0.5 μL) of transposon-transposase complex were mixed with 50 μl concentrated cells for electroporation (1.8kV, 200 Ω, 25μF using a Biorad Gene Pulser). Insertion mutants were selected on TYE media supplemented with tetracycline (5–7.5 μg/mL) by overnight growth at 30˚, and then harvested and pooled. Two independent pools were created, each made up of approximately 80,000 independent mutants. A *pbpA*-minus transposon mutant pool was created by transforming one of the ADP1 mutant pools with a PCR fragment corresponding to the Δ*pbpA*::*kan* mutation found in MAY103, with selection for kanamycin resistance on minimal-succinate agar.

Tn-seq analysis

Tn-seq screens were carried out for cells grown on fosfomycin or aztreonam. For the fosfomycin screen, one of the ADP1 transposon mutant pools was plated on protective medium supplemented with 360 μg/mL fosfomycin at approximately $5x10^7$ and $5x10^8$ cells/plate, grown for 24 hours at 30˚C and harvested (two Tn-seq assays total). For the aztreonam Tn-seq screen, the Δ*pbpA*::*kan* transposon mutant pool was plated on protective medium supplemented with aztreonam (120 or 192 μg/mL) at ~$5X10^5$ and $1X10^7$ cells/plate, and cells were harvested at 24 and 48 hours (eight Tn-seq assays total). As controls, mutant pools were grown on protective medium lacking antibiotic. Tn-seq analysis was carried out using a terminal deoxynucleotidyl terminal transferase-based procedure [45].

To identify genes whose inactivation affected giant cell formation after fosfomycin or aztreonam treatment, combined read counts for insertions in nonessential genes (5 to 90% of predicted coding regions, normalized for total reads/sequencing run) were evaluated for each time point analyzed, and histograms of the ratios of the log2-transformed read counts of antibiotic-treated to the corresponding antibiotic-untreated cultures plotted. Genes whose mutants were significantly depleted or enriched under giant cell induction conditions were identified using normal distribution thresholds specified for each condition in Data Set S1, with genes identified in multiple independent experiments chosen for subsequent validation studies using constructed deletion mutations.

Supporting information

S1 Fig. Giant cell morphology. A., paired phase contrast and fluorescence images of giant cells of a strain expressing cytoplasmic green fluorescent protein (MAY118 or MAY119). **B.**, giant cells with peripheral wispy filaments and vesicles. Giant cells were induced by exposure of wild type (MAY101) to fosfomycin (192 μg/ml) for 20–24 h on protective agar and then suspended in protective medium for microscopy. Scale bar, 10 μm. Fluorescent imaging employed an EGFP/FITC/CY2/Alexa Fluor 488 Filter Set.
(TIFF)

S2 Fig. Mutations accelerating giant cell formation after aztreonam treatment. Deletions of three genes (Δ*dacA* (MAY111), Δ*ldtG* (MAY115) and Δ*ponA* (MAY105)) in a ΔPBP2 genetic background speed giant cell formation and lead to premature lysis on protective agar. Note that the three mutants have larger cells that the ΔPBP2 parent strain (MAY102) at 9 h, and have mostly lysed by 24 h. A Δ*mrcB* mutant (MAY113) exhibits relatively normal giant cell

formation under these conditions. The *dacA*, *ldtG* and *ponA* deletions reduced the aztreonam minimal inhibitory growth concentration 3–8 fold. Scale bar, 10 µm.
(TIFF)

S3 Fig. Blocking peptidoglycan recycling accelerates giant cell formation and lysis. The formation of giant cells induced by exposure to different antibiotics in protective agar is shown for a wild type control strain (ΔIS) (MAY116) and a mutant deleted of *nagZ*, a gene required for peptidoglycan recycling (encoding ß-N-acetyl-glucosaminidase) (MAY125). The mutation accelerates formation and lysis of giant cells upon fosfomycin treatment, and causes smaller but detectable increases in lysis at 24 h in the aztreonam and meropenem treatment conditions. The Δ*nagZ* mutation reduced the fosfomycin MIC four-fold. Scale bar, 10 µm.
(TIFF)

S4 Fig. ZipA⁻ PBP2⁻ double mutant cells are viable giant cell producers. Microcolonies of *zipA⁺* and Δ*zipA* cells with or without the PBP2 gene (*pbpA*) are shown after growth for 24 h on protective agarose pads. WT, MAY101; Δ*pbpA*, MAY102; Δ*zipA*::*kan*, MAY130; Δ*pbpA* Δ*zipA*::*kan*, MAY131. Scale bar, 10 µm.
(TIFF)

S5 Fig. Giant cell formation by LOS-minus mutants. Microcolones of bacteria grown 12 hours on protective agarose pads with and without fosfomycin (192 µg/ml) are shown. The wild-type control strain (MAY116) carries IS1236 1::*kan*. Scale bar, 10 µm.
(TIFF)

S6 Fig. Reverse phenocopy test. The figure compares the microcolonies of giant cells formed in response to fosfomycin and aztreonam treatment compared to deletion of their presumptive target genes (*murA* and *ftsI* respectively) in the absence of the antibiotics. Bacteria (MAY107, MAY109 and MAY112) were grown 24 hr, 30 ˚C on protective agar in the presence of fosfomycin (360 µg/ml) or aztreonam (192 µg/ml), or for 18 h, 30 ˚C following transformation with selection on protective agar with 20 µg/ml kanamycin to create the indicated deletion mutants. Scale bar, 10 µm.
(TIFF)

S1 Movie. Giant cell formation after deletion of *murA*. The field shows the growth two cells for 10 hours after spotting a wild type (MAY101) transformation mix with selection for a Δ*murA*::*kan* on protective agarose pads. The cell at the center appears to have obtained the mutagenic PCR fragment and is thus kanamycin resistant, whereas that at the upper right has not and growth is inhibited by the kanamycin. The center cell divides and gives off cells that enlarge into amorphous giant cells. The microcolony that forms also contains cells that retain their normal size and shape and are presumably kanamycin sensitive. These cells may originate from transformants with multiple chromosomes that segregate both mutant and wild type chromosomes. Some of the giant cells lyse, while others grow in an amorphous amoeboid fashion. Many of the giant cells show small membranous filaments and small vesicles at their surfaces. Imaging was conducted using a Nikon Ti-E inverted wide-field fluorescence microscope with a large format sCMOS camera (Andor NEO) and controlled by NIS-Elements. Following transformation, cells were inoculated onto 2% agarose pads made with protective minimal-succinate medium containing kanamycin (20 µg/ml) to select growth of cells carrying the deletion insert. Cells were imaged using brightfield illumination at 30˚ every 2 min for 10 hours, and images used to generate time-lapse videos of micro-colony development.
(MP4)

S1 Table. Deletion mutant giant cell formation.
(DOCX)

S1 Database. Genes depleted in fosfomycin Tn-seq of wild-type.
(XLSX)

S2 Database. Bacterial strains and primers.
(XLSX)

Acknowledgments

We thank Larry Gallagher for helpful comments on the manuscript.

Author Contributions

Investigation: Jeannie Bailey, Julie Cass, Joe Gasper, Ngoc-Diep Ngo.

Supervision: Paul Wiggins, Colin Manoil.

Writing – original draft: Jeannie Bailey, Colin Manoil.

Writing – review & editing: Jeannie Bailey, Julie Cass, Colin Manoil.

References

1. Lee SA, Gallagher LA, Thongdee M, Staudinger BJ, Lippman S, Singh PK, et al. General and condition-specific essential functions of Pseudomonas aeruginosa. Proc Natl Acad Sci U S A. 2015; 112 (16):5189–94. https://doi.org/10.1073/pnas.1422186112 PMID: 25848053

2. Peters JM, Colavin A, Shi H, Czarny TL, Larson MH, Wong S, et al. A Comprehensive, CRISPR-based Functional Analysis of Essential Genes in Bacteria. Cell. 2016; 165(6):1493–506. https://doi.org/10.1016/j.cell.2016.05.003 PMID: 27238023

3. Barbe V, Vallenet D, Fonknechten N, Kreimeyer A, Oztas S, Labarre L, et al. Unique features revealed by the genome sequence of Acinetobacter sp. ADP1, a versatile and naturally transformation competent bacterium. Nucleic Acids Res. 2004; 32(19):5766–79. https://doi.org/10.1093/nar/gkh910 PMID: 15514110

4. Caccamo PD, Brun YV. The Molecular Basis of Noncanonical Bacterial Morphology. Trends Microbiol. 2018; 26(3):191–208. https://doi.org/10.1016/j.tim.2017.09.012 PMID: 29056293

5. de Boer PA. Bacterial physiology: Life minus Z. Nat Microbiol. 2016; 1(8):16121. https://doi.org/10.1038/nmicrobiol.2016.121 PMID: 27573120

6. Young KD. Bacterial shape: two-dimensional questions and possibilities. Annu Rev Microbiol. 2010; 64:223–40. https://doi.org/10.1146/annurev.micro.112408.134102 PMID: 20825347

7. Pazos M, Peters K, Vollmer W. Robust peptidoglycan growth by dynamic and variable multi-protein complexes. Curr Opin Microbiol. 2017; 36:55–61. https://doi.org/10.1016/j.mib.2017.01.006 PMID: 28214390.

8. Typas A, Banzhaf M, Gross CA, Vollmer W. From the regulation of peptidoglycan synthesis to bacterial growth and morphology. Nat Rev Microbiol. 2011; 10(2):123–36. https://doi.org/10.1038/nrmicro2677 PMID: 22203377

9. Zhao H, Patel V, Helmann JD, Dorr T. Don't let sleeping dogmas lie: new views of peptidoglycan synthesis and its regulation. Mol Microbiol. 2017; 106(6):847–60. https://doi.org/10.1111/mmi.13853 PMID: 28975672

10. Du S, Lutkenhaus J. Assembly and activation of the Escherichia coli divisome. Mol Microbiol. 2017; 105 (2):177–87. https://doi.org/10.1111/mmi.13696 PMID: 28419603

11. Cho H, Uehara T, Bernhardt TG. Beta-lactam antibiotics induce a lethal malfunctioning of the bacterial cell wall synthesis machinery. Cell. 2014; 159(6):1300–11. https://doi.org/10.1016/j.cell.2014.11.017 PMID: 25480295

12. Lederberg J, St Clair J. Protoplasts and L-type growth of Escherichia coli. Journal of bacteriology. 1958; 75(2):143–60. PMID: 13513575

13. Bendezu FO, de Boer PA. Conditional lethality, division defects, membrane involution, and endocytosis in mre and mrd shape mutants of Escherichia coli. Journal of bacteriology. 2008; 190(5):1792–811. https://doi.org/10.1128/JB.01322-07 PMID: 17993535

14. Errington J, Mickiewicz K, Kawai Y, Wu LJ. L-form bacteria, chronic diseases and the origins of life. Philos Trans R Soc Lond B Biol Sci. 2016; 371(1707). https://doi.org/10.1098/rstb.2015.0494 PMID: 27672147

15. Joseleau-Petit D, Liebart JC, Ayala JA, D'Ari R. Unstable Escherichia coli L forms revisited: growth requires peptidoglycan synthesis. Journal of bacteriology. 2007; 189(18):6512–20. https://doi.org/10.1128/JB.00273-07 PMID: 17586646

16. Dorr T, Davis BM, Waldor MK. Endopeptidase-mediated beta lactam tolerance. PLoS Pathog. 2015; 11 (4):e1004850. https://doi.org/10.1371/journal.ppat.1004850 PMID: 25884840

17. Monahan LG, Turnbull L, Osvath SR, Birch D, Charles IG, Whitchurch CB. Rapid conversion of Pseudomonas aeruginosa to a spherical cell morphotype facilitates tolerance to carbapenems and penicillins but increases susceptibility to antimicrobial peptides. Antimicrob Agents Chemother. 2014; 58(4):1956–62. https://doi.org/10.1128/AAC.01901-13 PMID: 24419348

18. Adler HI, Terry CE, Hardigree AA. Giant cells of Escherichia coli. Journal of bacteriology. 1968; 95 (1):139–42. PMID: 4866096

19. Vinella D, Joseleau-Petit D, Thevenet D, Bouloc P, D'Ari R. Penicillin-binding protein 2 inactivation in Escherichia coli results in cell division inhibition, which is relieved by FtsZ overexpression. Journal of bacteriology. 1993; 175(20):6704–10. https://doi.org/10.1128/jb.175.20.6704-6710.1993 PMID: 8407846

20. Weaver AI, Murphy SG, Umans BD, Tallavajhala S, Onyekwere I, Wittels S, et al. Genetic Determinants of Penicillin Tolerance in Vibrio cholerae. Antimicrob Agents Chemother. 2018; 62(10). https://doi.org/10.1128/AAC.01326-18 PMID: 30061291

21. Elliott KT, Neidle EL. Acinetobacter baylyi ADP1: transforming the choice of model organism. IUBMB Life. 2011; 63(12):1075–80. https://doi.org/10.1002/iub.530 PMID: 22034222.

22. Metzgar D, Bacher JM, Pezo V, Reader J, Doring V, Schimmel P, et al. Acinetobacter sp. ADP1: an ideal model organism for genetic analysis and genome engineering. Nucleic Acids Res. 2004; 32 (19):5780–90. https://doi.org/10.1093/nar/gkh881 PMID: 15514111

23. Reams AB, Roth JR. Mechanisms of gene duplication and amplification. Cold Spring Harb Perspect Biol. 2015; 7(2):a016592. https://doi.org/10.1101/cshperspect.a016592 PMID: 25646380

24. Cuff LE, Elliott KT, Seaton SC, Ishaq MK, Laniohan NS, Karls AC, et al. Analysis of IS1236-mediated gene amplification events in Acinetobacter baylyi ADP1. Journal of bacteriology. 2012; 194(16):4395–405. https://doi.org/10.1128/JB.00783-12 PMID: 22707704

25. de Berardinis V, Vallenet D, Castelli V, Besnard M, Pinet A, Cruaud C, et al. A complete collection of single-gene deletion mutants of Acinetobacter baylyi ADP1. Mol Syst Biol. 2008; 4:174. https://doi.org/10.1038/msb.2008.10 PMID: 18319726

26. Seaton SC, Elliott KT, Cuff LE, Laniohan NS, Patel PR, Neidle EL. Genome-wide selection for increased copy number in Acinetobacter baylyi ADP1: locus and context-dependent variation in gene amplification. Mol Microbiol. 2012; 83(3):520–35. https://doi.org/10.1111/j.1365-2958.2011.07945.x PMID: 22211470.

27. Yao Z, Kahne D, Kishony R. Distinct single-cell morphological dynamics under beta-lactam antibiotics. Mol Cell. 2012; 48(5):705–12. https://doi.org/10.1016/j.molcel.2012.09.016 PMID: 23103254

28. Zhang G, Baidin V, Pahil KS, Moison E, Tomasek D, Ramadoss NS, et al. Cell-based screen for discovering lipopolysaccharide biogenesis inhibitors. Proc Natl Acad Sci U S A. 2018; 115(26):6834–9. https://doi.org/10.1073/pnas.1804670115 PMID: 29735709

29. Davies TA, Shang W, Bush K, Flamm RK. Affinity of doripenem and comparators to penicillin-binding proteins in Escherichia coli and Pseudomonas aeruginosa. Antimicrob Agents Chemother. 2008; 52 (4):1510–2. https://doi.org/10.1128/AAC.01529-07 PMID: 18250190

30. Goryshin IY, Jendrisak J, Hoffman LM, Meis R, Reznikoff WS. Insertional transposon mutagenesis by electroporation of released Tn5 transposition complexes. Nat Biotechnol. 2000; 18(1):97–100. https://doi.org/10.1038/72017 PMID: 10625401.

31. Greene NG, Fumeaux C, Bernhardt TG. Conserved mechanism of cell-wall synthase regulation revealed by the identification of a new PBP activator in Pseudomonas aeruginosa. Proc Natl Acad Sci U S A. 2018; 115(12):3150–5. https://doi.org/10.1073/pnas.1717925115 PMID: 29507210

32. Knight D, Dimitrova DD, Rudin SD, Bonomo RA, Rather PN. Mutations Decreasing Intrinsic beta-Lactam Resistance Are Linked to Cell Division in the Nosocomial Pathogen Acinetobacter baumannii. Antimicrob Agents Chemother. 2016; 60(6):3751–8. https://doi.org/10.1128/AAC.00361-16 PMID: 27067318

33. Powers MJ, Trent MS. Expanding the paradigm for the outer membrane: Acinetobacter baumannii in the absence of endotoxin. Mol Microbiol. 2018; 107(1):47–56. https://doi.org/10.1111/mmi.13872 PMID: 29114953

34. Rojas ER, Billings G, Odermatt PD, Auer GK, Zhu L, Miguel A, et al. The outer membrane is an essential load-bearing element in Gram-negative bacteria. Nature. 2018; 559(7715):617–21. https://doi.org/10.1038/s41586-018-0344-3 PMID: 30022160.

35. Bojkovic J, Richie DL, Six DA, Rath CM, Sawyer WS, Hu Q, et al. Characterization of an Acinetobacter baumannii lptD Deletion Strain: Permeability Defects and Response to Inhibition of Lipopolysaccharide and Fatty Acid Biosynthesis. Journal of bacteriology. 2015; 198(4):731–41. https://doi.org/10.1128/JB.00639-15 PMID: 26668262

36. Fumeaux C, Bernhardt TG. Identification of MupP as a New Peptidoglycan Recycling Factor and Antibiotic Resistance Determinant in Pseudomonas aeruginosa. MBio. 2017; 8(2). https://doi.org/10.1128/mBio.00102-17 PMID: 28351916

37. Gisin J, Schneider A, Nagele B, Borisova M, Mayer C. A cell wall recycling shortcut that bypasses peptidoglycan de novo biosynthesis. Nat Chem Biol. 2013; 9(8):491–3. https://doi.org/10.1038/nchembio.1289 PMID: 23831760.

38. Magnet S, Bellais S, Dubost L, Fourgeaud M, Mainardi JL, Petit-Frere S, et al. Identification of the L,D-transpeptidases responsible for attachment of the Braun lipoprotein to Escherichia coli peptidoglycan. Journal of bacteriology. 2007; 189(10):3927–31. https://doi.org/10.1128/JB.00084-07 PMID: 17369299

39. Magnet S, Dubost L, Marie A, Arthur M, Gutmann L. Identification of the L,D-transpeptidases for peptidoglycan cross-linking in Escherichia coli. Journal of bacteriology. 2008; 190(13):4782–5. https://doi.org/10.1128/JB.00025-08 PMID: 18456808

40. Hugonnet JE, Mengin-Lecreulx D, Monton A, den Blaauwen T, Carbonnelle E, Veckerle C, et al. Factors essential for L,D-transpeptidase-mediated peptidoglycan cross-linking and beta-lactam resistance in Escherichia coli. Elife. 2016; 5. https://doi.org/10.7554/eLife.19469 PMID: 27767957

41. Glover WA, Yang Y, Zhang Y. Insights into the molecular basis of L-form formation and survival in Escherichia coli. PLoS One. 2009; 4(10):e7316. https://doi.org/10.1371/journal.pone.0007316 PMID: 19806199

42. Ranjit DK, Jorgenson MA, Young KD. PBP1B Glycosyltransferase and Transpeptidase Activities Play Different Essential Roles during the De Novo Regeneration of Rod Morphology in Escherichia coli. Journal of bacteriology. 2017; 199(7). https://doi.org/10.1128/JB.00612-16 PMID: 28096447

43. Zeytuni N, Zarivach R. Structural and functional discussion of the tetra-trico-peptide repeat, a protein interaction module. Structure. 2012; 20(3):397–405. https://doi.org/10.1016/j.str.2012.01.006 PMID: 22404999.

44. Cambre A, Zimmermann M, Sauer U, Vivijs B, Cenens W, Michiels CW, et al. Metabolite profiling and peptidoglycan analysis of transient cell wall-deficient bacteria in a new Escherichia coli model system. Environ Microbiol. 2015; 17(5):1586–99. https://doi.org/10.1111/1462-2920.12594 PMID: 25142185.

45. Gallagher LA, Ramage E, Weiss EJ, Radey M, Hayden HS, Held KG, et al. Resources for Genetic and Genomic Analysis of Emerging Pathogen Acinetobacter baumannii. Journal of bacteriology. 2015; 197 (12):2027–35. https://doi.org/10.1128/JB.00131-15 PMID: 25845845

46. Miller JH. Experiments In Molecular Genetics. Cold Spring Harbor, New York: Cold Spring Harbor Press; 1972.

47. Leong CG, Boyd CM, Roush KS, Tenente R, Lang KM, Lostroh CP. Succinate, iron chelation, and monovalent cations affect the transformation efficiency of Acinetobacter baylyi ATCC 33305 during growth in complex media. Can J Microbiol. 2017; 63(10):851–6. https://doi.org/10.1139/cjm-2017-0393 PMID: 28772085.

48. Palmen R, Vosman B, Buijsman P, Breek CK, Hellingwerf KJ. Physiological characterization of natural transformation in Acinetobacter calcoaceticus. J Gen Microbiol. 1993; 139(2):295–305. https://doi.org/10.1099/00221287-139-2-295 PMID: 8436948.

49. Chang AC, Cohen SN. Construction and characterization of amplifiable multicopy DNA cloning vehicles derived from the P15A cryptic miniplasmid. Journal of bacteriology. 1978; 134(3):1141–56. PMID: 149110